

Supporting Information

Ru-Doping and Conductive Metal-Organic-Frameworks Co-Modification Strategy for Enhanced Full Water Splitting Performance of CoCu-LDH Nanosheets Array

Saiya Guo^{#,a} Wentao Lin^{#,a} Manman Shi,^a Jieding Wei,^a Wei Che,^b Jong-Beom Baek,^b and Yonghong Ni^{a*}

^a College of Chemistry and Materials Science, Key Laboratory of Functional Molecular Solids, Ministry of Education, Anhui Laboratory of Molecule-Based Materials, Anhui Normal University, 189 Jiuhua Southern Road, Wuhu, 241002, PR. China. Email: niyh@mail.ahnu.edu.cn (Y.H. Ni)

^b Ulsan National Institute of Science and Technology (UNIST), School of Energy and Chemical Engineering/Center for Dimension-Controllable Organic Frameworks, 50 UNIST, Ulsan 44919, South Korea. Email: nanoche@mail.ustc.edu.cn (W. Che)

[#] Saiya Guo and Wentao Lin contributed equally.

Material Characterizations: The phases of the products were characterized by the X-ray powder diffraction technology. The data were collected on a Rigaku SmartLab Studio II X-ray diffractometer equipped with Cu K α radiation ($\lambda = 0.15406$ nm), employing a scanning rate of $20^\circ \text{ min}^{-1}$ in the 2θ range from 3 to 80° . Field emission scanning electron microscopy (FESEM) images of the products were carried out on a Hitachi Regulus-8100 field emission scanning electron microscope, employing an accelerating voltage of 5 kV. Transmission electron microscopy (TEM) images were obtained on a Hitachi HT7700 transmission electron microscope with an accelerating voltage of 120 kV. The HAADF-STEM and elemental mapping images were obtained on a Thermo Scientific Talos F200E scanning transmission electron microscope. The X-ray photoelectron spectra

(XPS) of the samples were examined by Thermo ESCALAB 250 spectroscopy instrument with a monochromatic Al K α ($h\nu = 1486.6$ eV) at the power of 150 W. On the Shimadzu Model FTIR-8400s spectrometer, a small number of samples and KBr (SP) were pressed into thin slices, and the Fourier transform infrared (FT-IR) spectra of the samples were recorded. The contact angle experiments were performed on a surface analyzer (Theta, Attention) with 4 μ L 1 M KOH droplet at room temperature. Inductively coupled plasma mass spectrometry (ICP-OES) was tested on Optima 7300 DV (Perkin Elmer Corporation).

Electrochemical Measurements: All electrochemical measurements were conducted by a standard three electrode system (CHI660e, CH instrument, Shanghai, China) at room temperature with 1 M KOH electrolyte (pH is about 13.8). The graphite rod and the standard Hg/HgO served as the counter electrode and the reference electrodes, respectively. All samples were grown on the CF substrate (2 cm \times 1 cm) and used as working electrodes directly. The measured potential was converted into RHE according to the following equation: $E_{(RHE)} = E_{(Hg/HgO)} + (0.098 + 0.059 \times pH)$ V. E_{RHE} represents the voltage relative to the standard reversible hydrogen electrode, $E_{Hg/HgO}$ refers to the reference voltage tested in the experiment, and all measurements were performed at room temperature. Before testing, the electrocatalyst was cycled in the potential ranges from -0.9 to -1.4 V (vs Hg/HgO) until a steady CV curve was obtained. Linear sweep voltammetry (LSV) was tested with 85% iR compensation at a scan rate of 5 mV s $^{-1}$. To evaluate the intrinsic behavior of as-synthesized self-supported electrocatalysts, iR correction was used to exclude the influence of Ohmic resistance and the contribution of the capacitance of the CF was calibrated. Furthermore, the kinetic reaction mechanism was calculated from the Tafel equation:

$$\eta = b \log j + a \quad (S1)$$

Electrochemically active surface areas (ECSA) were calculated by dividing the double layer capacitance (C_{dl}) with specific capacitance of these samples. C_{dl} was determined by measuring cyclic voltammograms (CVs) with multiple scan rates in non-faradaic potential region. CV curves were measured at various scan rates from 20 to 100 mV·s $^{-1}$ under the potential window from 0.427 to 0.527 V (vs RHE). According to the followed equation, the ECSA of the catalyst were calculated:

$$ECSA = C_{dl}/C_s \quad (C_s \text{ is a constant, here equals } 0.04 \text{ mF cm}^{-2}) \quad (S2)$$

EIS spectra were obtained in a frequency range of 100 kHz to 0.01 Hz at the overpotential of -

0.083 V (vs RHE), and the EIS results were presented in the form of Nyquist plot. The durability was performed through the chronopotentiometry measurement at -50 mA cm^{-2} .

The Faradaic efficiency of CoCuRu-HHTP/CoCuRu-LDH was evaluated using a two-electrode system in 1 M KOH solution. The H_2 and O_2 gas generated in the Hoffman instrument was collected using a water drainage method. The Faraday efficiency was calculated by comparing the theoretical values with experimental ones.

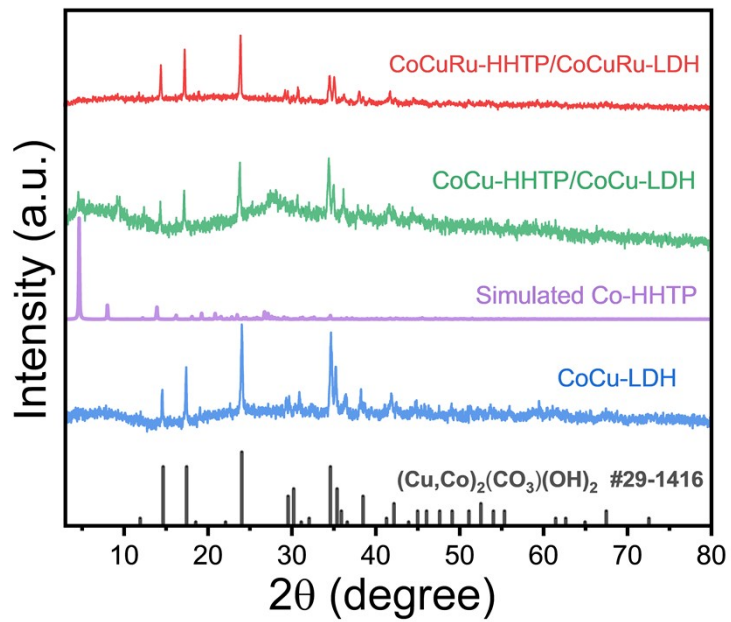


Figure S1. XRD patterns of as-prepared CoCu-LDH, CoCu-HHTP/CoCu-LDH and CoCuRu-HHTP/CoCuRu-LDH samples, and simulated XRD pattern of Co-HHTP.

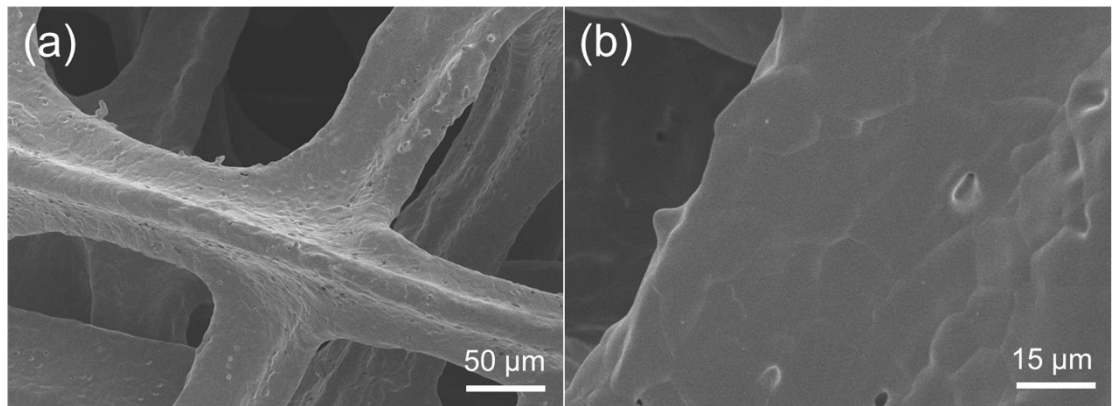


Figure S2. (a) low-magnification and (b) high-magnification SEM images of CF substrate.

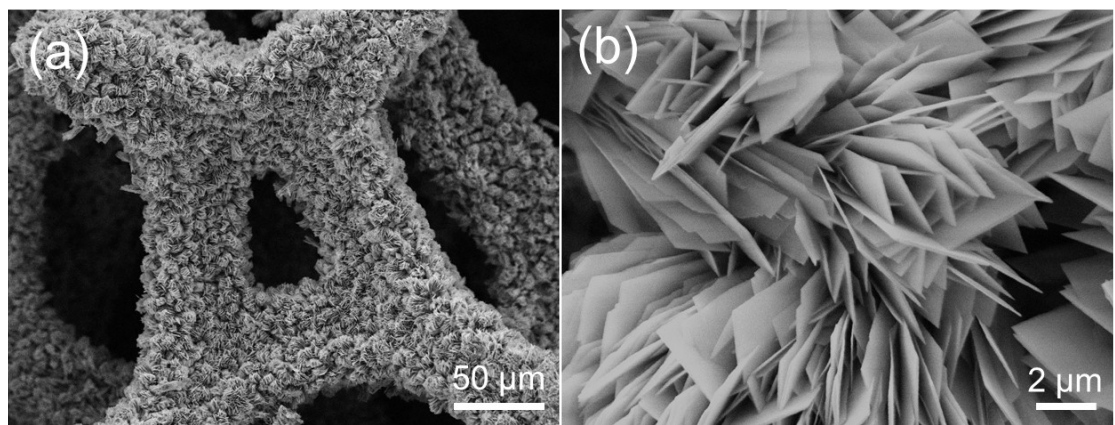


Figure S3. (a) low-magnification and (b) high-magnification SEM images of the as-prepared CoCu-LDH nanosheets array.

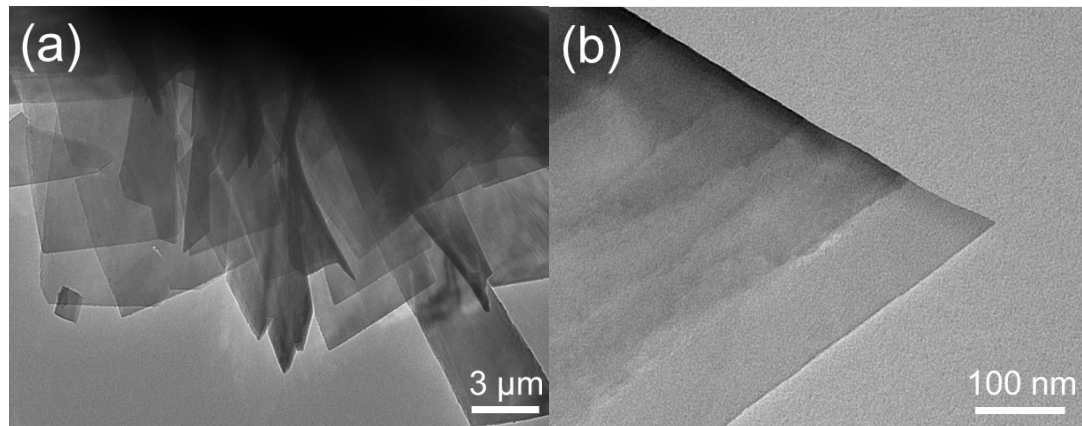


Figure S4. (a) low-magnification and (b) high-magnification TEM images of the as-prepared CoCu-LDH nanosheets.

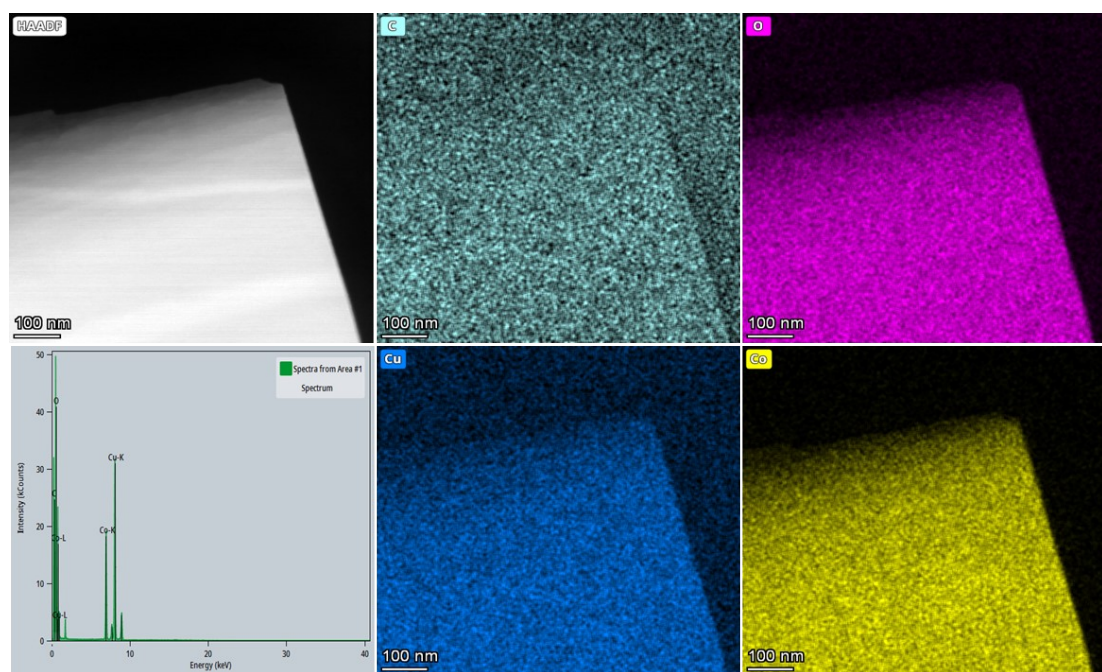


Figure S5. EDS analysis and element mapping images of C, O, Cu, Co in CoCu-LDH nanosheets.

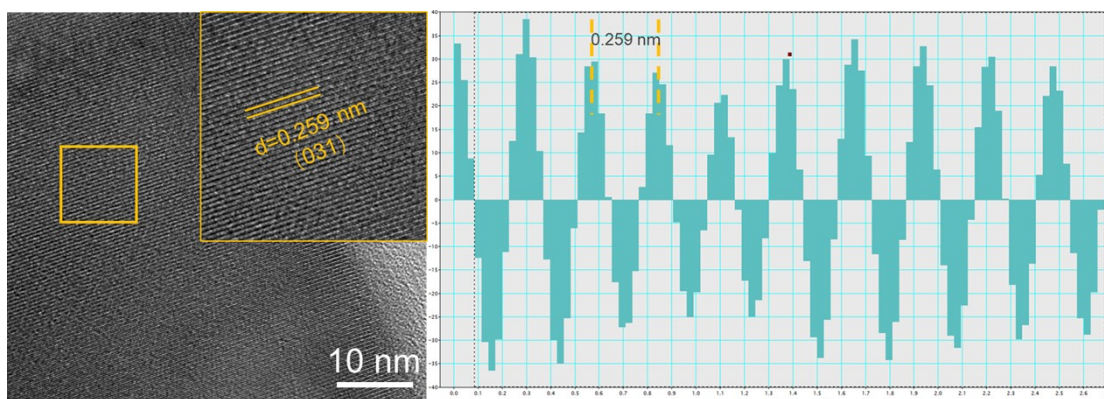


Figure S6. HRTEM images of a CoCu-LDH nanosheet.

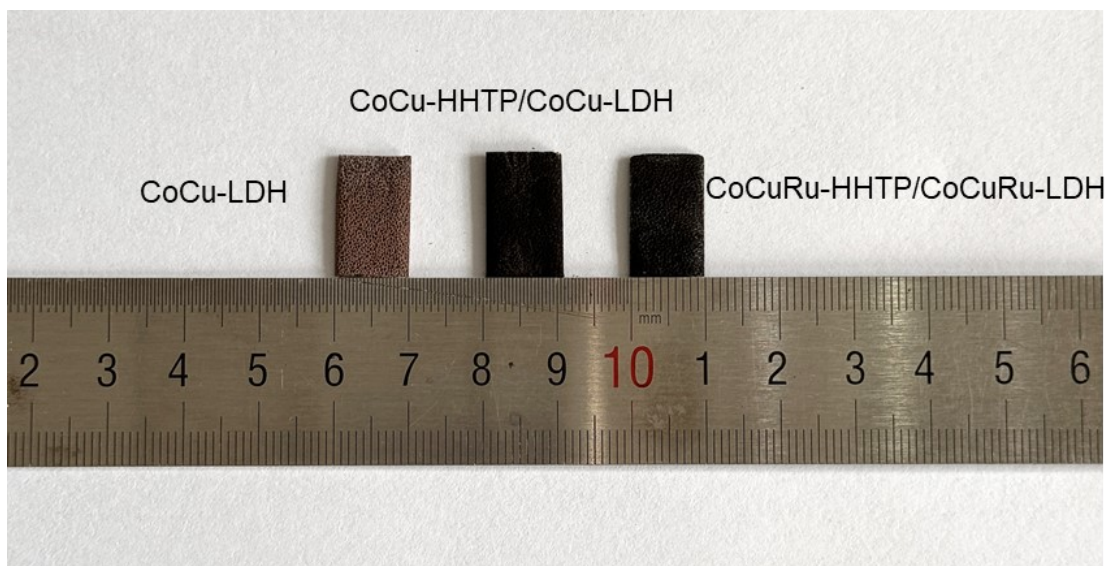


Figure S7. Optical pictures of CoCu-LDH, CoCu-HHTP/CoCu-LDH and CoCuRu-HHTP/CoCuRu-LDH with the size of $1.0 \text{ cm} \times 1.5 \text{ cm}$ on CF substrate, which were trimmed for electrochemical testing.

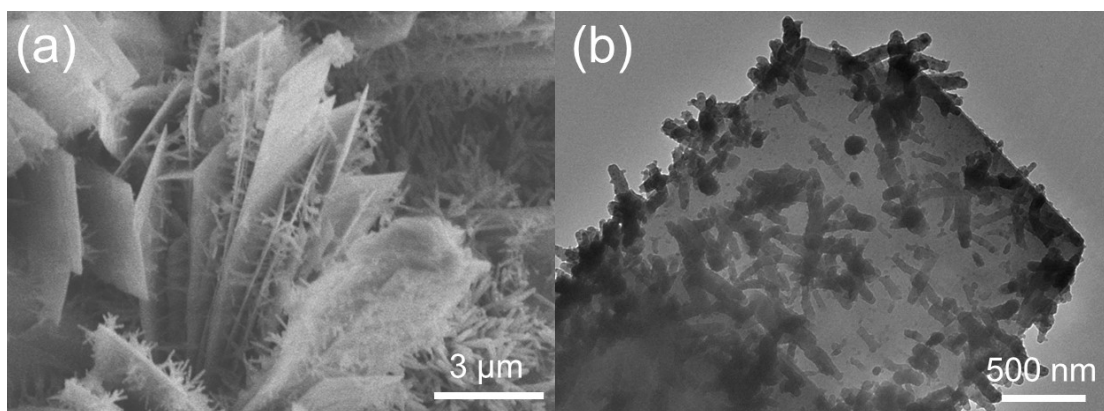


Figure S8. (a) SEM and (b) TEM images of as-prepared CoCu-HHTP/CoCu-LDH nanosheets.



Figure S9. Optical photograph of the solution before and after Ru^{3+} exchange.

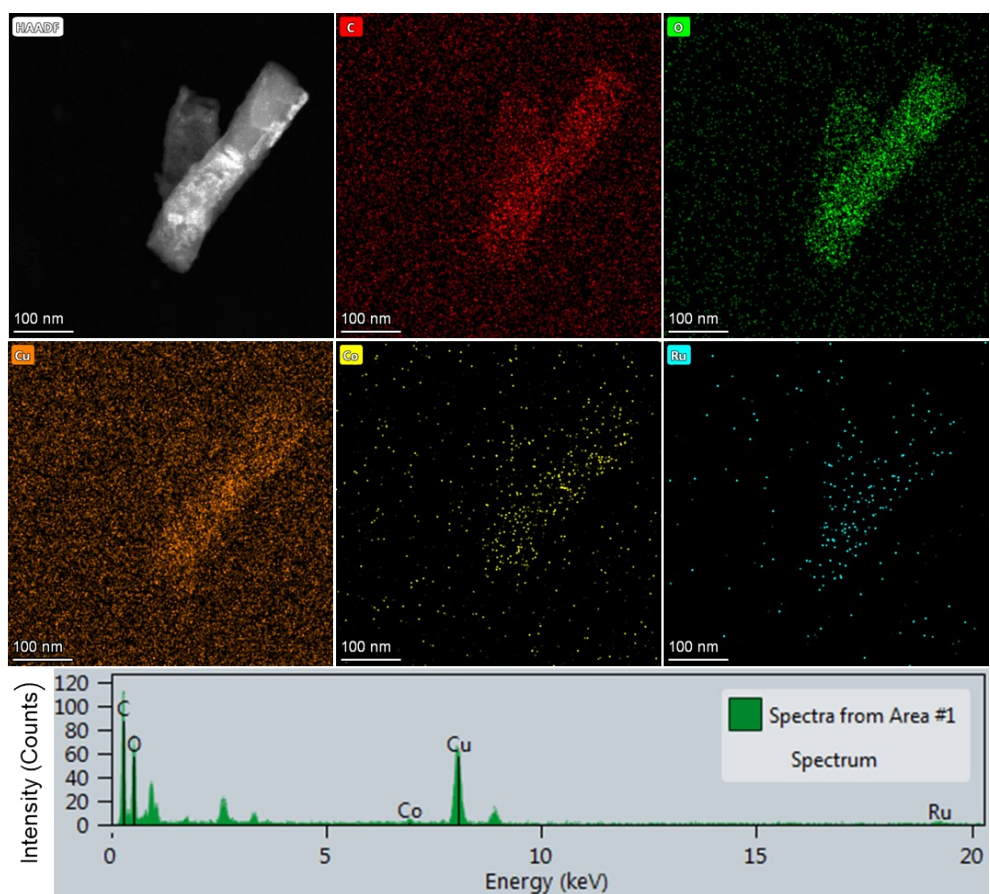


Figure S10. The EDS analysis of rod-like nanostructures (MOF) exfoliated from the nanosheets by ultrasound and the corresponding element mapping images.

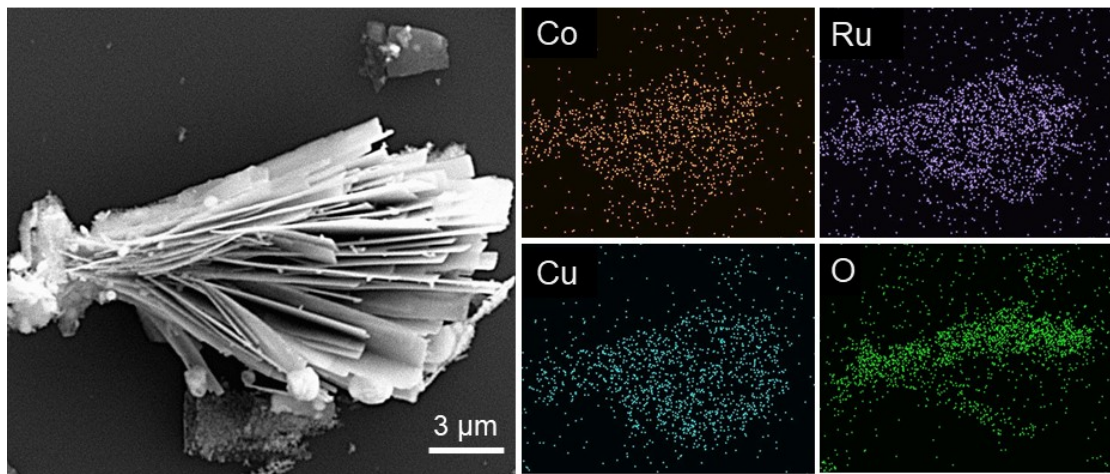


Figure S11. The element mapping images of CoCuRu-LDH.

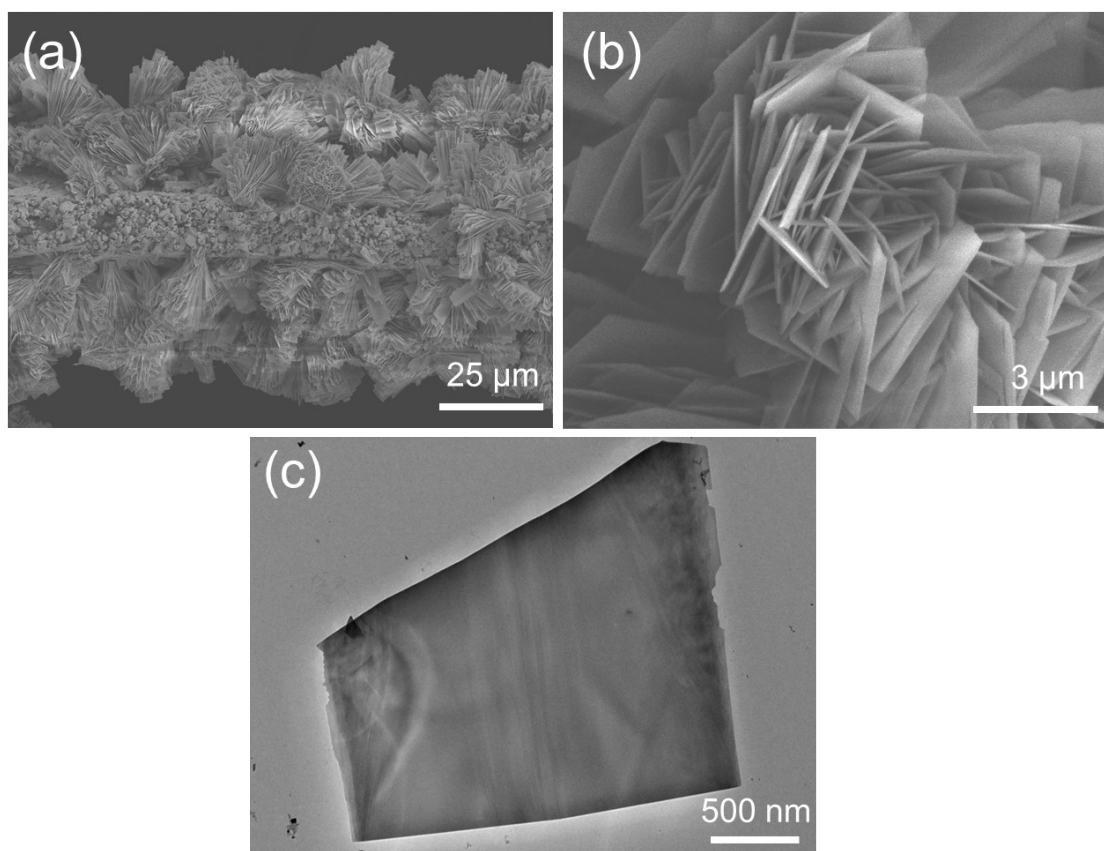


Figure S12. Electron microscopy images of CoCuRu-LDH nanosheets: (a) Low-magnification and (b) high-magnification SEM images, (c) TEM image.

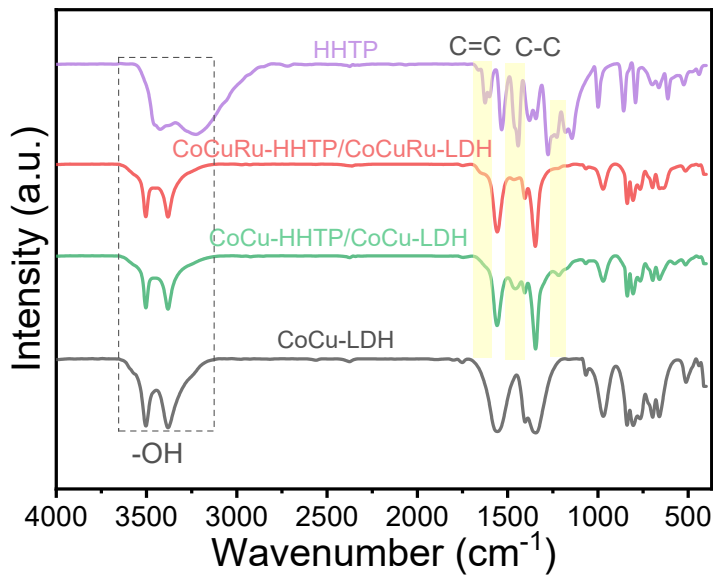


Figure S13. FT-IR spectra of HHTP, CoCuRu-HHTP/CoCuRu-LDH, CoCu-HHTP/CoCu-LDH and CoCu-LDH.

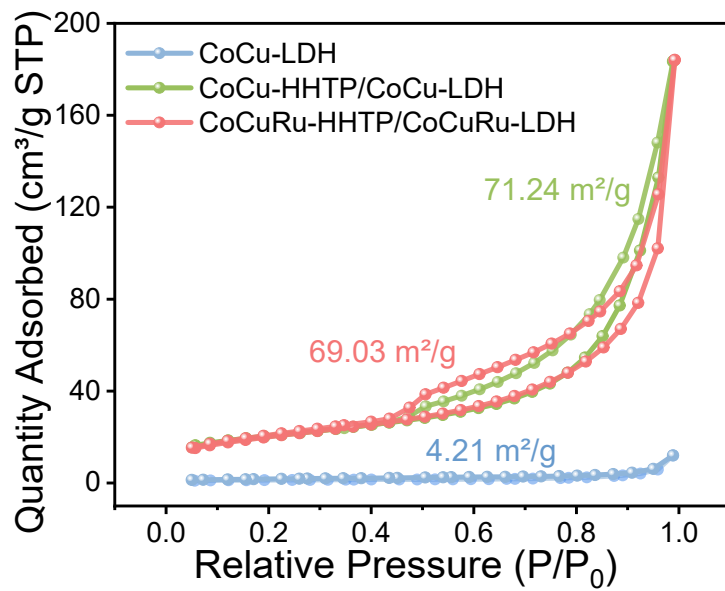


Figure S14. N₂ adsorption-desorption isotherms of CoCu-LDH, CoCu-HHTP/CoCu-LDH and CoCuRu-HHTP/CoCuRu-LDH.

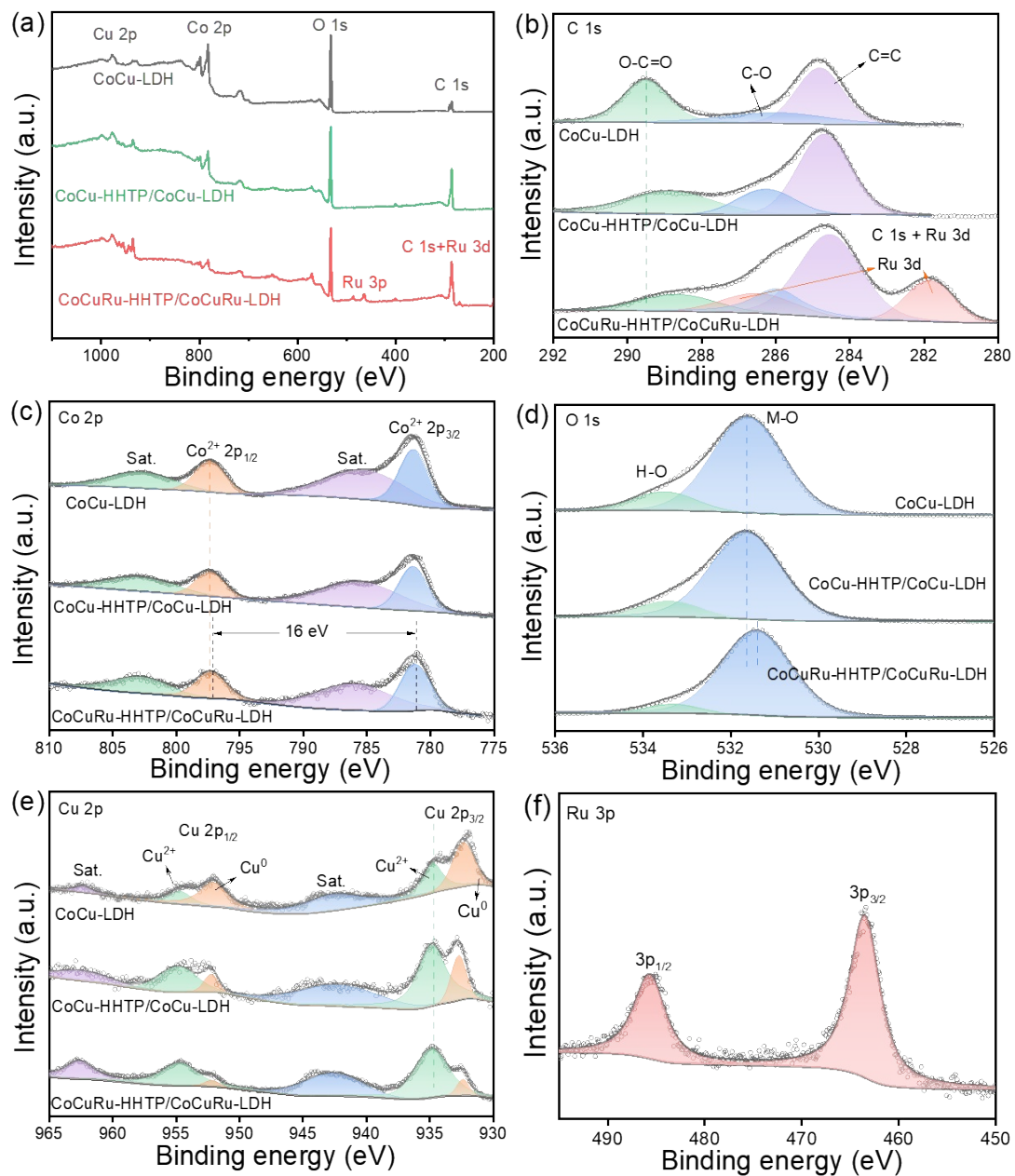


Figure S15. (a) XPS survey spectra of the products prepared at different stages and (b-e) high resolution spectra of C 1s (b), Co 2p (c), O 1s (d), Cu 2p (e). (f) High resolution XPS spectrum of Ru 3p in CoCuRu-HHTP/CoCuRu-LDH.

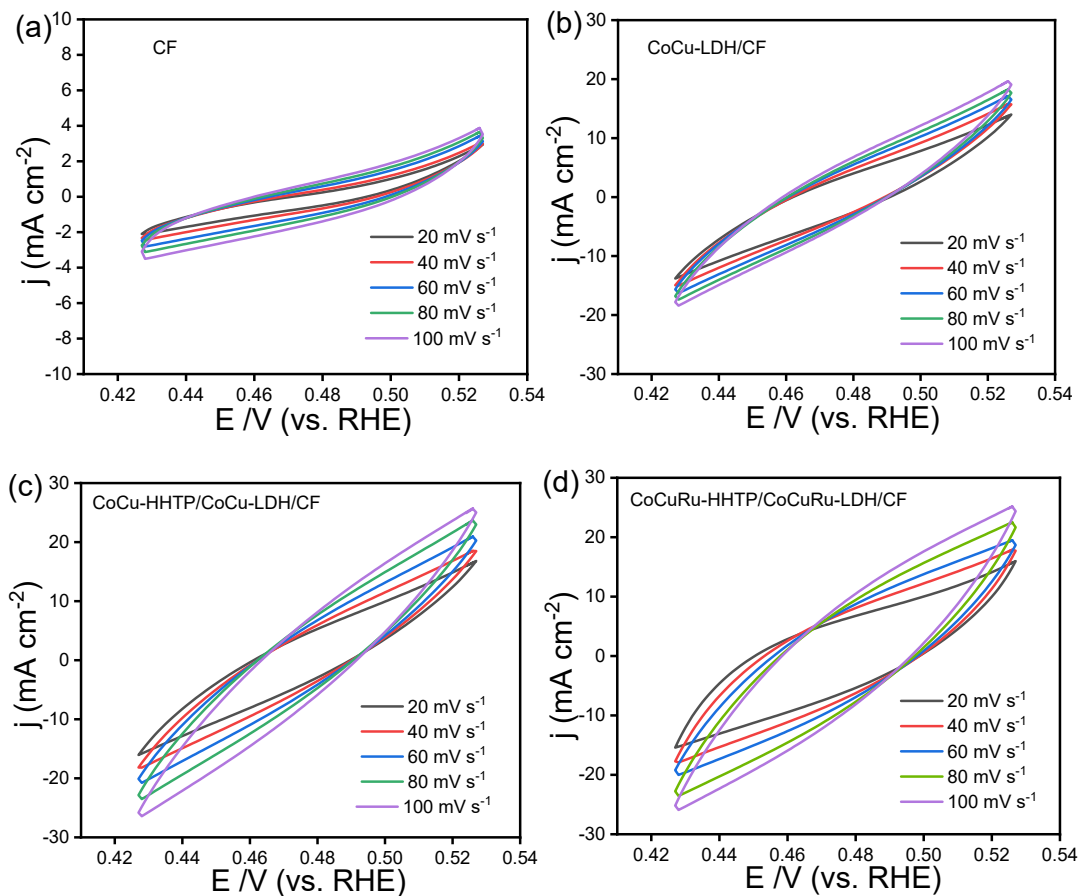


Figure S16. CV curves of various electrodes at different scan rates of 20, 40, 60, 80 and 100 mV s^{-1} for HER: (a) CF, (b) CoCu-LDH/CF, (c) CoCu-HHTP/CoCu-LDH/CF and (d) CoCuRu-HHTP/CoCuRu-LDH/CF.

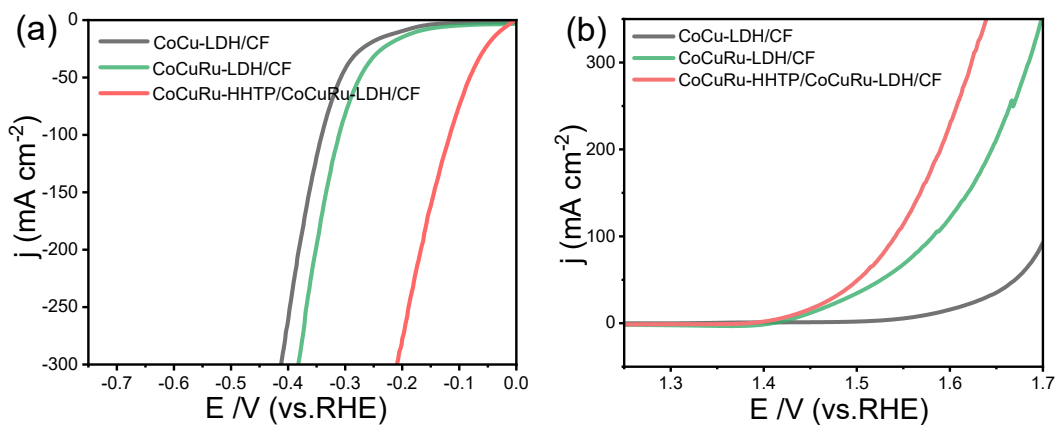


Figure S17. LSV curves of CoCu-LDH/CF, CoCuRu-LDH/CF and CoCuRu-HHTP/CoCuRu-LDH/CF electrodes for (a) HER and (b) OER.

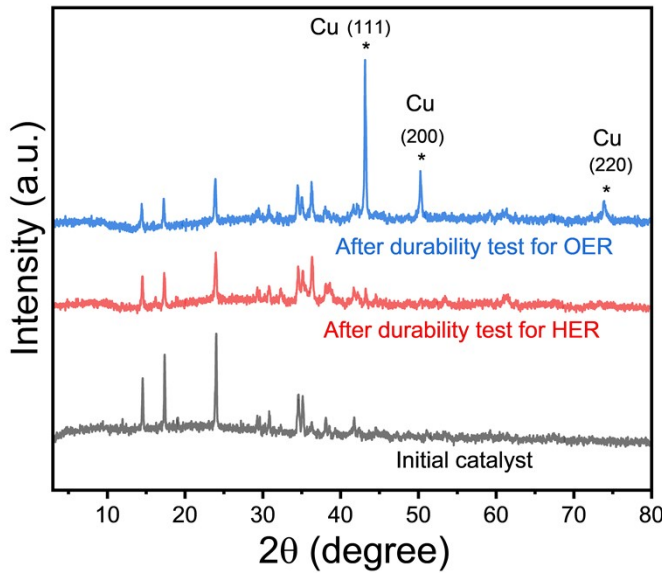


Figure S18. XRD patterns of CoCuRu-HHTP/CoCuRu-LDH before and after durability tests. (The Cu⁰ peak is due to the mixing of Cu foam substrate fragments with the catalyst powder during ultrasonic collection of the sample.)

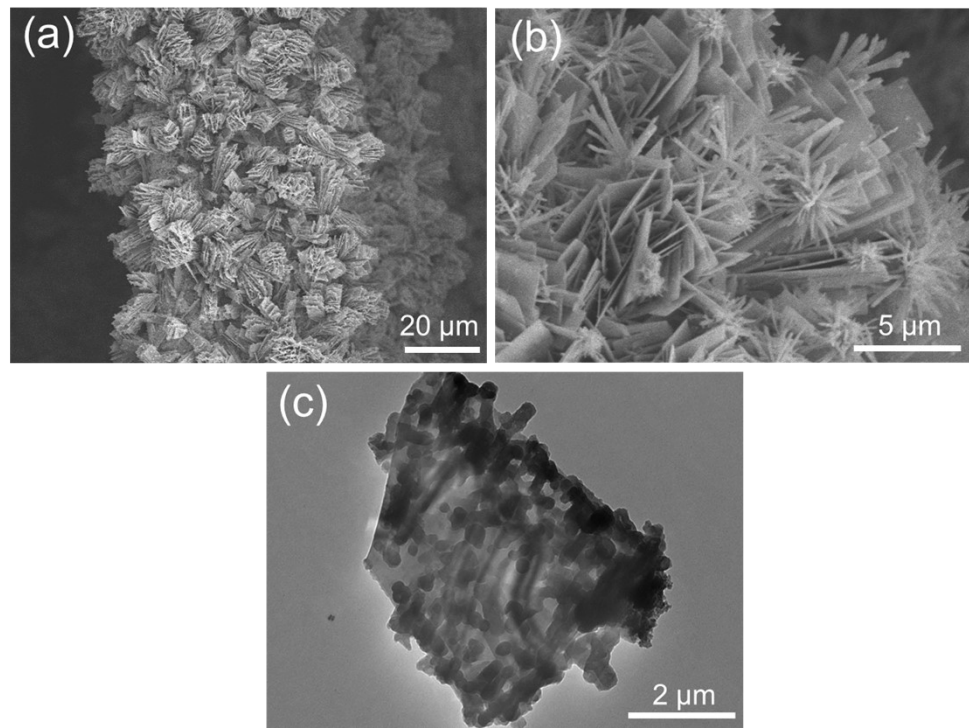


Figure S19. (a) Low- and (b) high-magnification SEM images, and (c) TEM image of CoCuRu-HHTP/CoCuRu-LDH after 150 h of durability test for HER.

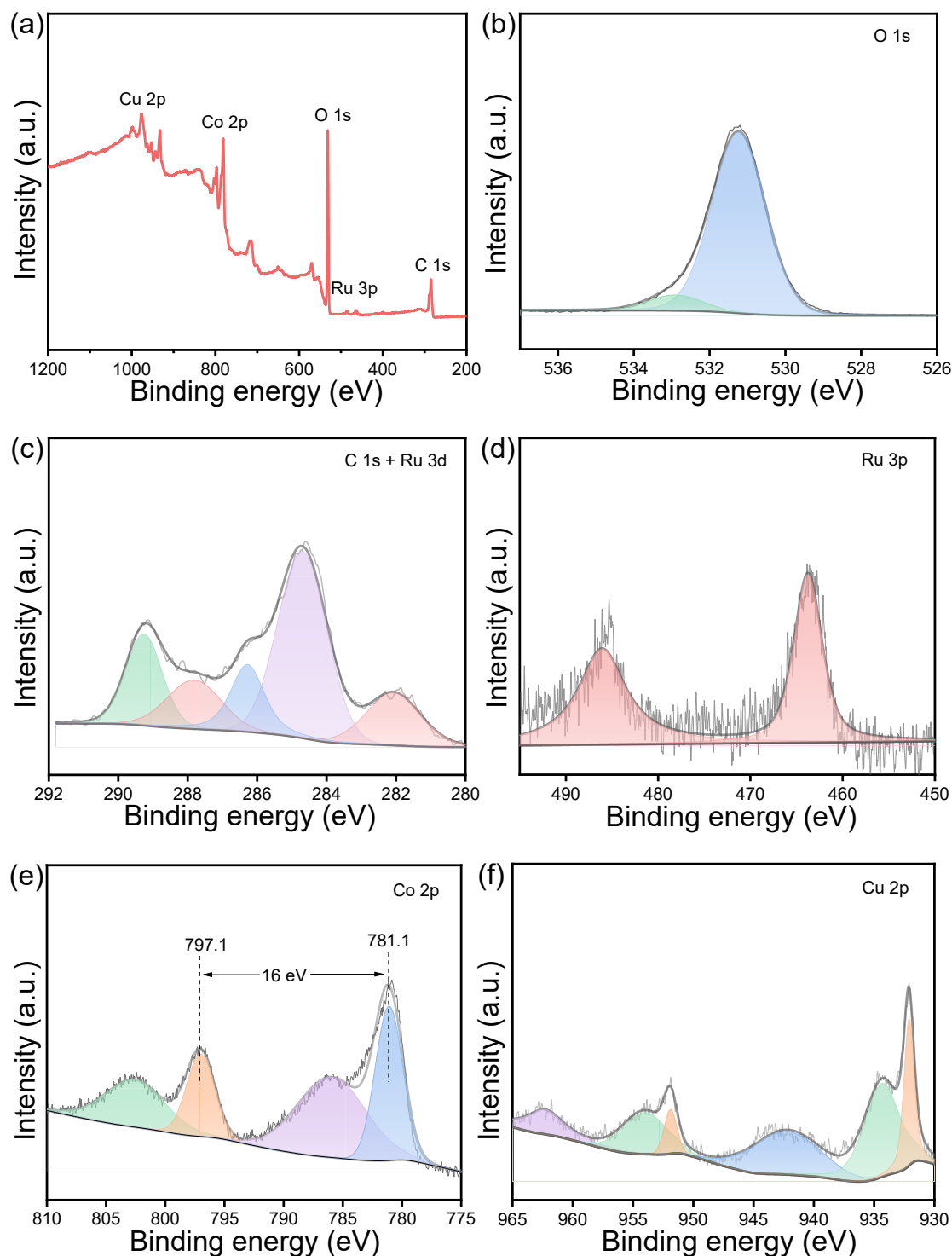


Figure S20. XPS analyses of CoCuRu-HHTP/CoCuRu-LDH after 150 h of durability test for HER: (a) survey spectrum, (b) O 1s, (c) C 1s+Ru 3d, (d) Ru 3p, (e) Co 2p and (f) Cu 2p.

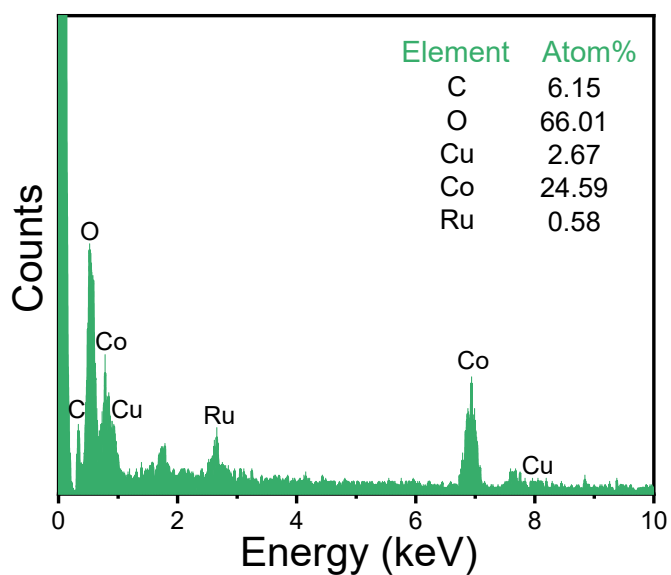


Figure S21. EDS analysis of CoCuRu-HHTP/CoCuRu-LDH after 150 h of durability test for HER.

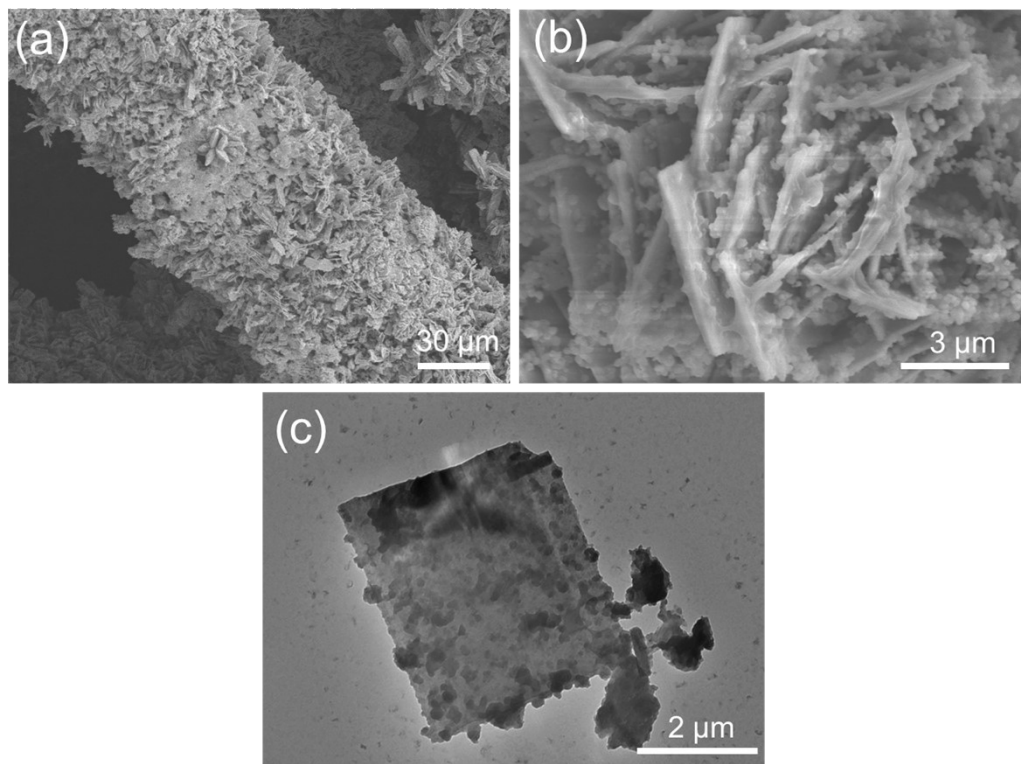


Figure S22. (a) Low- and (b) high-magnification SEM images, and (c) TEM image of CoCuRu-HHTP/CoCuRu-LDH after 120 h of durability test for OER.

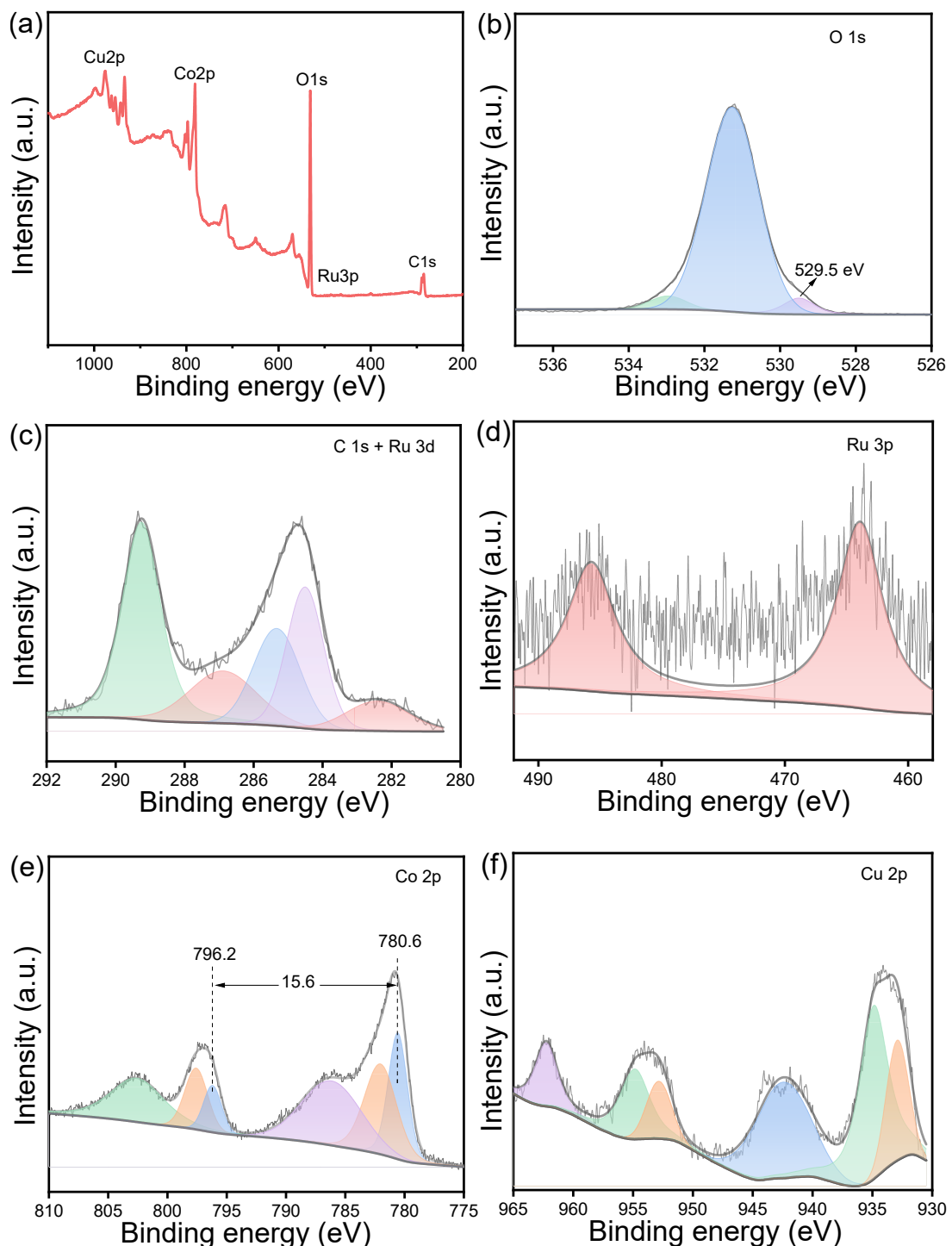


Figure S23. XPS analyses of CoCuRu-HHTP/CoCuRu-LDH after 120 h of durability test for OER: (a) survey spectrum, (b) O 1s, (c) C 1s+Ru 3d, (d) Ru 3p, (e) Co 2p and (f) Cu 2p.

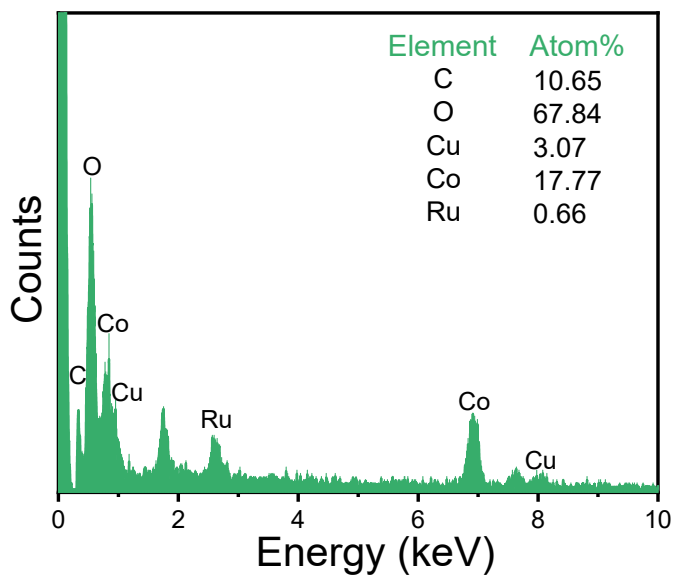


Figure S24. EDS analysis of CoCuRu-HHTP/CoCuRu-LDH after 120 h of durability test for OER.



Figure S25. The photograph of the as-used Hoffman instrument.

Table S1. The ICP analysis of the solution after Ru³⁺ exchange.

Sample	Element	Atom ratio (%)
Solution after ion exchange	Co	8.79
	Cu	28.12
	Ru	63.09

Table S2. The mass percentages for different samples from ICP analyses.

Sample	Element	Mass ratio (%)
CoCu-LDH	Co	46.79
	Cu	10.47
CoCu-HHTP/CoCu-LDH	Co	48.45
	Cu	8.768
CoCuRu-HHTP/CoCuRu-LDH	Co	42.28
	Cu	5.630
	Ru	1.855

Table S3. Comparison of HER activities of other catalysts in 1 M KOH solution.

Sample	η (mV)		Tafel slope (mV dec ⁻¹)	Ref.
	10 mA·cm ⁻²	100 mA·cm ⁻²		
CoCuRu-HHTP/CoCuRu-LDH	27	114	55.77	This work
CoNiRu-NT	22	124	78	1
Mo-RuCoOx	41	77	24.3	2
Ru@Cr-FeMOF	21	\	25.91	3
Ni ₂ P/FeP-FF	42	207	39.6	4
NiCoP	56	128	88.9	5
RuO ₂ /Co ₃ O ₄	53	177	48.85	6
RuIrOx	13	\	23	7
Ru@Ni-MOF	22	\	121	8
NiRu _{0.13} -BDC	36	132	36	9
CoRu-BPDC	37	103	73.22	10
MXene@RuCoNPs	20	\	30.4	11
Fe(OH) _x @Cu-MOF	112	\	76	12
Ni ₂ P/MoS ₂ -CoMo ₂ S ₄ @C	73	170	46.3	13
Mo _{ACs} /N-Ti ₃ C ₂ T _x	60	\	56	14
Fe _{1.2} (CoNi) _{1.8} Se ₆ MESe	66		66	15

Table S4. Comparison of OER activities of other catalysts in 1 M KOH solution.

Sample	η (mV)		Tafel slope (mV dec ⁻¹)	Ref.
	10 mA·cm ⁻²	100 mA·cm ⁻²		
CoCuRu-HHTP/CoCuRu-LDH	204	312	53.46	This work
Ni ₂ P/FeP-FF	217	250	31.90	4
RuO ₂ /Co ₃ O ₄	213	381	65.67	6
RuIrOx	250	\	42	7
MXene@RuCoNPs	353	309	61.30	11
Fe _{1.2} (CoNi) _{1.8} Se ₆ MESe	216	286	49	15
ZnFeNiCuCoRu-O	170	\	56	16
FeOOH@NiFe LDH	255	\	51.49	17
Ni ₃ (HITP) ₂	390	\	67	18
NiCo LDH-TPA	267	\	52.40	19
Ru-MnFeP/NF	191	\	69	20
Ni _{cluster} -Ru NWs	194	\	59	21
Co-COF@MOF	328	\	43.23	22
P-CeSAs@CoO	261	\	75	23
CoFe-CDs	320	\	84.90	24
MS-Co _{SA} -N-C-800°C	320	\	94.20	25

Table S5. Comparison of some bifunctional catalysts for overall water splitting activities in 1 M KOH solution.

Sample	Cell voltage (V)	Cell voltage (V)	Ref.
	10 mA·cm ⁻²	100 mA·cm ⁻²	
CoCuRu-HHTP/CoCuRu-LDH	1.48	1.64	This work
CoNiRu-NT	1.47	1.96	1
Mo-RuCoO _x	1.457	\	2
Ni ₂ P/FeP-FF	\	1.69	4
NiCoP	\	1.652	5
RuO ₂ /Co ₃ O ₄ (RCO)	\	1.50	6
MXene@RuCoNPs	1.52	\	11
Ni ₂ P/MoS ₂ -CoMo ₂ S ₄ @C	1.45	\	13
Fe _{1.2} (CoNi) _{1.8} Se ₆ MESe	1.55	\	15
RuCu NSs	1.49	\	26
MoO ₃ /Ni-NiO	1.55	\	27
Co ₄ N-CeO ₂ /GP	1.51	\	28
Fe-CoP/Ni(OH) ₂	1.52	1.59	29
Pt@LDH	1.49	\	30
CoVRu LDH	1.52	\	31
RuFe@NF	1.54	\	32
Ru-FeRu@C/NC	1.63	\	33
Ru-H ₂ O/CC-350	1.67	\	34

References

- Y. Wang, S. Wang, Z. L. Ma, L. T. Yan, X. B. Zhao, Y. Y. Xue, J. M. Huo, X. Yuan, S. N. Li, Q. G. Zhai, *Adv. Mater.*, 2022, **34**, 2107488.
- Y. J. Zhang, R. H. Lu, C. Wang, Y. Zhao, L. M. Qi, *Adv. Funct. Mater.*, 2023, **33**, 2303073.
- C. F. Zhao, J. Wang, Y. Gao, J. Zhang, C. Y. Huang, Q. H. Shi, S. Mu, Q. Xiao, S. Huo, Z. H.

- Xia, J. J. Zhang, X. G. Lu, Y. F. Zhao, *Adv. Funct. Mater.*, 2023, **34**, 2307917.
- 4. M. Jiang, H. H. Zhai, L. B. Chen, L. Mei, P. F. Tan, K. Yang, J. Pan, *Adv. Funct. Mater.*, 2023, **33**, 2302621.
 - 5. D. Chen, H. W. Bai, J. W. Zhu, C. Wu, H. Y. Zhao, D. L. Wu, J. X. Jiao, P. X. Ji, S. C. Mu, *Adv. Energy Mater.*, 2023, **13**, 2300499.
 - 6. Q. H. Su, R. Sheng, Q. C. Liu, J. Ding, P. Y. Wang, X.C. Wang, J. L. Wang, Y. G. Wang, B. Wang, Y. D. Huang, *J. Colloid Interface Sci.*, 2024, **658**, 43-51.
 - 7. Z. W. Zhuang, Y. Wang, C. Q. Xu, S. J. Liu, C. Chen, Q. Peng, Z. B. Zhuang, H. Xiao, Y. Pan, S. Q. Lu, R. Yu, W. C. Cheong, X. Cao, K. L. Wu, K. A. Sun, Y. Wang, D. S. Wang, J. Li, Y. D. Li, *Nat. Commun.*, 2019, **10**, 4875.
 - 8. L. Deng, F. Hu, M. Ma, S. C. Huang, Y. Xiong, H. Y. Chen, L. Li, S. Peng, *Angew. Chem., Int. Ed.*, 2021, **60**, 22276-22282.
 - 9. Y. Sun, Z. Xue, Q. Liu, Y. Jia, Y. Li, K. Liu, Y. Lin, M. Liu, G. Li, C. Y. Su, *Nat. Commun.*, 2021, **1**, 1369.
 - 10. X. Li, D. Luo, F. Jiang, K. Zhang, S. Wang, S. Li, Q. Zha, Y. Huang, Y. Ni, *Small*, 2023, **19**, 2301850.
 - 11. J. Li, C. Hou, C. Chen, W. Ma, Q. Li, L. Hu, X. Lv, J. Dang, *ACS Nano* 2023, **17**, 10947-10957.
 - 12. W. R. Cheng, H. B. Zhang, D. Y. Luan, X. W. Lou, *Sci. Adv.*, 2021, **7**, abg2580.
 - 13. F. C. Pan, J. Jia, F. Gong, Y. Liu, S. Liu, S. C. Jun, D. Lin, Y. Guo, Y. Yamauchi, Y. Huo, *ACS Nano*, 2024, **18**, 6202-6214.
 - 14. P. F. Wu, Y. Q. Yang, H. Y. Xi, Y. Si, Y. H. Chu, X. Z. Su, W. S. Yan, T. T. You, Y. K. Gao, Y. Wang, W. X. Chen, Y. Y. Huang, P. G. Yin, *Small*, 2023, **20**, 202306716.
 - 15. H. Wu, Z. C. Wang, Z. X. Li, Y. J. Ma, F. Ding, F. Q. Li, H. F. Bian, Q. X. Zhai, Y. L. Ren, Y. X. Shi, Y. R. Yang, Y. Deng, S. C. Tang, X. K. Meng, *Adv. Energy Mater.*, 2023, **13**, 2300837.
 - 16. K. Miao, W. Jiang, Z. Chen, Y. Luo, D. Xiang, C. Wang, X. Kang, *Adv. Mater.*, 2023, **36**, 202308490.
 - 17. Y. Li, Y. Wu, M. Yuan, H. Hao, Z. Lv, L. Xu, B. Wei, *Appl. Catal., B Environ.*, 2022, **318**, 121825.

18. X. H. Liu, Y. W. Yang, X. M. Liu, Q. Hao, L. M. Wang, B. Sun, J. Wu, D. Wang, *Langmuir*, 2020, **36**, 7528-7532.
19. W. Liu, D. Zheng, T. Deng, Q. Chen, C. Zhu, C. Pei, H. Li, F. Wu, W. Shi, S. W. Yang, Y. H. Zhu, X. H. Cao, *Angew. Chem., Int. Ed.*, 2021, **60**, 10614-10619.
20. D. Chen, Z. H. Pu, R. H. Lu, P. X. Ji, P. Y. Wang, J. W. Zhu, C. Lin, H. W. Li, X. G. Zhou, Z. Y. Hu, F. J. Xia, J. S. Wu, S. C. Mu, *Adv. Energy Mater.*, 2020, **10**, 202000814.
21. T. Zhu, S. Liu, B. Huang, Q. Shao, M. Wang, F. Li, X. Tan, Y. Pi, S. C. Weng, B. Huang, Z. Hu, J. Wu, Y. Qian, X. Huang, *Energy Environ. Sci.*, 2021, **14**, 3194-3202.
22. Z. Guo, S. Yang, M. Liu, Q. Xu, G. Zeng, *Small* 2023, **20**, 2308598.
23. M. Li, X. Wang, K. Liu, H. Sun, D. Sun, K. Huang, Y. Tang, W. Xing, H. Li, G. Fu, *Adv. Mater.*, 2023, **35**, 202302462.
24. M. Yang, T. Feng, Y. Chen, J. Liu, X. Zhao, B. Yang, *Appl. Catal., B Environ.*, 2020, **267**, 118657.
25. K. Wang, Z. Lu, J. Lei, Z. Liu, Y. Li, Y. Cao, *ACS Nano*, 2022, **16**, 11944-11956.
26. Q. Yao, B. Huang, N. Zhang, M. Sun, Q. Shao, X. Huang, *Angew., Chem., Int. Ed.*, 2019, **131**, 14121-14126.
27. X. Li, Y. Wang, J. Wang, Y. Da, J. Zhang, L. Li, C. Zhong, Y. Deng, X. Han, W. Hu, *Adv. Mater.*, 2020, **3**, 202003414.
28. H. Sun, C. Tian, G. Fan, J. Qi, Z. Liu, Z. Yan, F. Cheng, J. Chen, C. P. Li, M. Du, *Adv. Funct. Mater.*, 2020, **30**, 1910596.
29. X. Yu, J. Zhao, M. Johnsson, *Adv. Funct. Mater.*, 2021, **31**, 2101578.
30. J. M. Huo, Z. L. Ma, Y. Wang, Y. J. Cao, Y. C. Jiang, S. N. Li, Y. Chen, M. C. Hu, Q. G. Zhai, *Small*, 2023, **19**, 2207044.
31. K. Zeng, M. Tian, X. Chen, J. Zhang, M. H. Rummeli, P. Strasser, J. Sun, R. Yang, *Chem. Eng. J.*, 2023, **452**, 139151.
32. H. Liu, Q. Jia, S. Huang, L. Yang, S. Wang, L. Zheng, D. Cao, *J. Mater. Chem. A*, 2022, **10**, 4817-4824.
33. W. Feng, Y. Feng, J. Chen, H. Wang, Y. Hu, T. Luo, C. Yuan, L. Cao, L. Feng, J. Huang, *Chem. Eng. J.*, 2022, **437**, 135456.
34. M. You, X. Du, X. Hou, Z. Wang, Y. Zhou, H. Ji, L. Zhang, Z. Zhang, S. Yi, D. Chen, *Appl.*

